Excited state nonlinear optics of quasi-one-dimensional Mott-Hubbard insulators

Haranath Ghosh*
Max Planck Institute for the Physics of Complex Systems, Nöthnitzer Straße 38, 01187 Dresden, Germany
and Laser Physics Application Division, Raja Ramanna Centre for Advanced Technology, Indore 452013, India
(Received 5 March 2007; published 29 June 2007)

Ground as well as excited state nonlinear optical properties of one-dimensional Mott-Hubbard insulators are discussed in detail. One-dimensional strongly correlated materials are predicted to have several orders of magnitude larger *excited state* optical nonlinearities in comparison to that from the ground state. Unlike π-conjugated polymers and other classes of one-dimensional systems, strongly correlated materials such as Sr_2CuO_3, halogen-bridged Ni compounds, etc., have excited one- and two-photon allowed states almost energetically degenerate, which leads to order(s)-of-magnitude larger dipole coupling between them in comparison to that between the ground and optical states. This causes several orders of magnitude enhancement in the optical nonlinearities obtained from the first two-photon state in the wavelength region suitable for terahertz communications. Our results and conclusions are based on exact numerical calculations of the extended Hubbard model suitable for strongly correlated systems. We argue based on theoretical as well as available experimental data that one-dimensional cuprates would be a good source of terahertz radiation, to be experimentally verified. We also discuss in detail ground state nonlinear properties such as third-harmonic generation, two-photon absorption, and electroabsorption from the theoretical model and compare with experiments. Theoretical calculations of excited state nonlinearities of some π-conjugated polymers are also presented for comparison.

DOI: 10.1103/PhysRevB.75.235127 PACS number(s): 71.27.+a, 42.65.−k, 78.20.Bh, 78.47.+p

I. INTRODUCTION

Electron-electron correlation in condensed-matter systems exhibited a large number of wonders such as superconductivity, magnetism, giant magnetoresistance, and many others;[1] enhanced optical nonlinearity is also proved to be the manifestations of strong Coulomb repulsion among conducting electrons together with quantum confinement.[2–5] Research on nonlinear optics of strongly correlated one-dimensional systems originated from Refs. 2 and 3, both of which principally showed the occurrence of nearly degenerate one- and two-photon states due to strong Coulomb correlation. These nearly degenerate one- and two-photon states are also strongly dipole coupled. This was also the reason for strong optical nonlinearity obtained through two-photon absorption (TPA), electroreflectance spectra of these compounds, and analyzed theoretically. Spin-charge separation on Sr_2CuO_3 system[4,6–8] and joint influence of charge-transfer gap and on-site[5] repulsion were emphasized. Potential of Sr_2CuO_3 single crystals as a nonlinear optical material for all-optical switching devices was pointed out.[9] Similarly, for halogen-bridged nickel chain compounds, ultrafast optical switching to a metallic state by photoinduced Mott transition was reported.[10] Further important developments such as evidence of two types of charge-transfer excitations in Sr_2CuO_3 were found from electron-energy-loss spectroscopy analysis.[11] Higher-dimensional counterparts of these materials (e.g., $Sr_2CuO_2Cl_2$) are found to have an order of magnitude lower optical nonlinearity.[12,13,21] Even then such stimulating science and application research in one dimension has also led to the study of nonlinear optical properties in higher-dimensional Mott-Hubbard systems[14] too. Furthermore, femtosecond spectroscopic studies in quasi-two-dimensional cuprates[14] revealed strong role played by magnetic excitations in ultrafast nonradiative relaxation processes, which are related to the large Heisenberg exchanges in cuprates.

Subsequently, large third-order optical nonlinearity in one-dimensional Cu-O chain systems such as Sr_2CuO_3 and Ca_2CuO_3 was investigated by third-harmonic generation (THG) spectroscopy;[15] some of these results were reconfirmed by A. Maeda *et al.*,[16] by Z-scan technique, and by M. Ono *et al.*,[17] along with detailed studies on Ni-halogen chain compounds. There are some discrepancies in these studies too which we discuss later. One dominant one-photon peak at $\omega_A=0.61$ eV and a two-photon resonant peak $\omega_B=0.87$ eV were observed together with an *oscillatory structure* at $\omega_C \sim 2\omega_B$ and $\omega_A \simeq 2\omega_B/3$, in the case of Sr_2CuO_3. Thus, the one-photon state is at energy $0.61\times 3=1.83$ eV, whereas the two-photon state is at $0.87\times 2=1.74$ eV—the two-photon state is below the one-photon state. This observation is contrary to the other earlier studies, where the two-photon state is above the one-photon state.[2,3] We shall show that this energy ordering of low-energy excited states is extremely significant for photoinduced absorption (PA), excited state optical nonlinearities, etc. Furthermore, determination of locations of one- and two-photon states obtained in Ref. 3 by three-level system fitting procedure seems to be doubtful because we shall show that the concerned two-photon state corresponds to the dip of the Im $\chi^{(3)}(-\omega;0,0,\omega)$. On the contrary, locations of two-photon states in Refs. 3 and 17 appear to be away from the dip of Im $\chi^{(3)}(-\omega;0,0,\omega)$. This would lead to the fact that the energy difference between the one- and two-photon states would be even smaller than predicted and might be reverse ordered as well similar to the observation in Ref. 15. These would further shed light on the mechanism of gigantic nonlinearities in these materials.

In this paper, one of our prime interests is theoretical prediction of huge *excited state* optical nonlinearities compared

to that from the ground state in these classes of materials. Here, first we theoretically demonstrate the observed THG spectrum and that the oscillatory structure at ω_C is another higher-energy two-photon state which can be verified experimentally. We also present TPA, electroabsorption (EA), and PA theoretically and compare with available experimental data. These results of ground state nonlinear as well as linear properties compare well with experiments. Then, we consider the case of third-order nonlinear optical susceptibilities from an excited state rather than the ground state to predict a general enhancement[18] in one-dimensional (1D) Mott-Hubbard insulators. We predict from our theoretical calculation that these classes of materials would have *several orders of magnitude larger* excited state optical nonlinearities (e.g., excited state THG, TPA, EA) compared to that from the ground state. We emphasize that this is an artifact of strongly correlated nature of these systems—π-conjugated polymers can also have about 2 orders of magnitude larger excited state optical nonlinearity compared to that of the ground state. So far, it was well known that π-conjugated organic molecules and polymer systems are of interest due to the delocalized π-electron systems which give rise to large values of $\chi^{(3)}$, but one-dimensional Mott-Hubbard systems, on the contrary, are not so delocalized but dominated by electron-electron repulsion. Furthermore, choice of large optical nonlinear medium depends not only on the ground state but also on the excited state matter.[19] Nonlinear optical materials with large third-order nonlinear susceptibilities, fast response time, low loss, and operability at room temperature are indispensable for next generation all-optical switching, computing devices, because the magnitudes of these quantities strongly influence the instrument performance. One of the pioneering experimental demonstration of excited state enhancement of optical nonlinearities was by Rodenberger *et al.* in linear conjugated molecules,[18] showing around 2 orders of magnitude enhancement in nonlinearity. 50- to 160-fold increase in third-order nonlinearity was also observed in bacteriochlorophylls.[20] However, there are no studies yet on excited state nonlinearities on one-dimensional Mott-Hubbard insulators (as mentioned earlier), and given earlier experimental demonstrations in π-conjugated organic molecules,[18,20] we hope that experimental verification of our theoretical predictions will also be possible. We also predict that at least one-dimensional Cu-O chain systems may be used as a source for terahertz radiation source. This is because the lowest two-photon electronic state is below the one-photon state and energetically degenerate.

The rest of the paper is organized as follows. In Sec. II, we describe a short method of the numerical calculation of the extended Hubbard model suitable for Mott-Hubbard systems. In Sec. III, we present detailed results of ground state linear as well as nonlinear optical properties. In Sec. IV, excited state nonlinear properties and their general enhancement mechanism are discussed. A short discussion on phenyl based π-conjugated polymers is also presented in this section. Detailed summary of all results and conclusions are drawn in Sec. V.

II. THEORETICAL MODEL CALCULATION

One of the most widely used theoretical model for studying strongly correlated electron system is known as the Hubbard model. One-dimensional Mott-Hubbard insulators that we are concerned about are Sr_2CuO_3, Ca_2CuO_3, and $[Ni(chxn)_2X]Y_2$ where $X \equiv$ halogen (such as Cl, Br, etc.), chxn $\equiv$ cylohexanediamine, and $Y \equiv$ counterion such as Cl, Br, NO_3. One-dimensional Cu-O chains are composed of CuO_4 quadrilateral structures with shared corner oxygens, in which the Cu ion is divalent (spin quantum number $S=1/2$) and one unpaired electron exists in the overlap of the p_x, p_y orbitals of O and the $d_{x^2-y^2}$ orbitals of Cu. Because of large on-site Coulomb repulsion energy U_{Cu} (described below) acting on Cu ions, the Mott-Hubbard gap is opened in the Cu $3d_{x^2-y^2}$ band. The occupied O $2p$ band is located between the Cu $3d$ upper Hubbard band and Cu $3d$ lower Hubbard band. Similarly, in the case of halogen-bridged Ni hallides, Ni^{3+} ions and X^- are arranged alternately along the chain axis, forming purely 1D electronic state composed of the p_z orbitals of X and the d_{z^2} orbitals of the Ni. Four N atoms of amino groups in two chxn molecules coordinate a Ni^{3+} ion in a plane normal to the chain axis and produce a strong ligand field. A Ni^{3+} ion is therefore in a low-spin state (d^7; $S=1/2$) and one unpaired electron exists in the d_{z^2} orbital. Thus, both the cuprates as well as the halogen-bridged Ni compounds described above are one-dimensional Mott-Hubbard insulators [involving two different kinds of bands Cu(Ni) $3d_{x^2-y^2}(3d_{z^2})$ and O(X) $2p_{x,y}(2p_z)$]. Therefore, we use two band extended Hubbard model corresponding to Cu $3d_{x^2-y^2}$ (Ni $3d_{z^2}$) and O $p_{x,y}$(X p_z) as below.

$$H = \sum_{\langle ij\rangle,\sigma} t_{ij}(c^{\dagger}_{i\sigma}c_{j\sigma} + \mathrm{H.c.}) + \sum_{i\sigma}(-1)^i \epsilon n_i + \sum_i U_i n_{i\uparrow} n_{i\downarrow} + \sum_i V n_i n_{i+1}. \quad (1)$$

The first term of the above equation represents hopping probability between Cu(Ni) and O(X) sites. The second term represents the on-site energies of the Cu(Ni) and O(X) and thereby defining the charge-transfer energy $2\epsilon = \epsilon_{\mathrm{O}(X)} - \epsilon_{\mathrm{Cu(Ni)}}$. The third term represents the most dominant term in the Hamiltonian known as the on-site Coulomb repulsion, the energy felt by two electrons occupying the same Cu (Ni)3d or O (X) p orbital with opposite spins. The fourth term is known as the intersite Coulomb repulsion (V), the repulsive energy felt by two electrons occupying the neighboring Cu (Ni) and O (X) sites. We solve this Hamiltonian exactly numerically for a ring of 12 sites containing six Cu (Ni) and six O (X) sites. Within wide existing literature for oxides, we studied extensively various combinations of a set of parameter values, $|t|=0.75-1.4$ eV, $U_{\mathrm{Cu(Ni)}}=10-8$ eV, $U_{\mathrm{O}(X)}=6-4$ eV, $\epsilon=0.5-2.0$ eV, $V=0.5-3$ eV, that satisfies the well-known value of the exchange integral $J \sim 2300-2800$ K,[21] suitable for cuprates as well as Ni hallides.

The technique used here is an exact diagonalization method using second quantized valence bond technique originally developed by Mazumdar and co-workers[22] and later by Ramasesha *et al.*[23] We follow the same notations of Dixit and Mazumdar.[22] We describe briefly on the same basis for smaller system size that can also be solved exactly ana-

lytically. Imagine a ring of Cu-O-Cu-O in which odd (even) sites correspond to Cu (O). For a four-site ring problem, the following configurations are possible in the even-parity subspace:

$$|\phi_{1+}\rangle = \begin{pmatrix} 1 & 0 \\ 0 & 1 \end{pmatrix},$$

$$|\phi_{2+}\rangle = \frac{1}{2}\left[\begin{pmatrix} 0 & 1 \\ 0 & 1 \end{pmatrix} + \begin{pmatrix} 1 & 0 \\ 1 & 0 \end{pmatrix} + \begin{pmatrix} 1 & 1 \\ 0 & 0 \end{pmatrix} + \begin{pmatrix} 0 & 0 \\ 1 & 1 \end{pmatrix}\right],$$

$$|\phi_{3+}\rangle = \frac{1}{\sqrt{2}}\left[\begin{pmatrix} 2 & 0 \\ 0 & 0 \end{pmatrix} + \begin{pmatrix} 0 & 0 \\ 0 & 2 \end{pmatrix}\right],$$

$$|\phi_{4+}\rangle = \frac{1}{\sqrt{2}}\left[\begin{pmatrix} 0 & 2 \\ 0 & 0 \end{pmatrix} + \begin{pmatrix} 0 & 0 \\ 2 & 0 \end{pmatrix}\right],$$

$$|\phi_{5+}\rangle = \begin{pmatrix} 0 & 1 \\ 1 & 0 \end{pmatrix}.$$

Correspondingly, the odd-parity subspace would contain the following configurations:

$$|\phi_{1-}\rangle = \frac{1}{2}\left[\left\{\begin{pmatrix} 0 & 1 \\ 0 & 1 \end{pmatrix} + \begin{pmatrix} 1 & 0 \\ 1 & 0 \end{pmatrix}\right\} - \left\{\begin{pmatrix} 1 & 1 \\ 0 & 0 \end{pmatrix} + \begin{pmatrix} 0 & 0 \\ 1 & 1 \end{pmatrix}\right\}\right],$$

$$|\phi_{2-}\rangle = \frac{1}{\sqrt{2}}\left[\begin{pmatrix} 2 & 0 \\ 0 & 0 \end{pmatrix} - \begin{pmatrix} 0 & 0 \\ 0 & 2 \end{pmatrix}\right],$$

$$|\phi_{3-}\rangle = \frac{1}{\sqrt{2}}\left[\begin{pmatrix} 0 & 2 \\ 0 & 0 \end{pmatrix} - \begin{pmatrix} 0 & 0 \\ 2 & 0 \end{pmatrix}\right],$$

$$|\phi_{4-}\rangle = \frac{1}{2}\left[\left\{\begin{pmatrix} 0 & 1 \\ 0 & 1 \end{pmatrix} + \begin{pmatrix} 1 & 1 \\ 0 & 0 \end{pmatrix}\right\} - \left\{\begin{pmatrix} 1 & 0 \\ 1 & 0 \end{pmatrix} + \begin{pmatrix} 0 & 0 \\ 1 & 1 \end{pmatrix}\right\}\right],$$

$$|\phi_{5-}\rangle = \frac{1}{2}\left[\left\{\begin{pmatrix} 0 & 1 \\ 0 & 1 \end{pmatrix} + \begin{pmatrix} 0 & 0 \\ 1 & 1 \end{pmatrix}\right\} - \left\{\begin{pmatrix} 1 & 0 \\ 1 & 0 \end{pmatrix} + \begin{pmatrix} 1 & 1 \\ 0 & 0 \end{pmatrix}\right\}\right],$$

where the configurations

$$|\phi\rangle \equiv \begin{pmatrix} 1 & 2 \\ 3 & 4 \end{pmatrix}$$

actually represents occupations in various sites (1,2,…). Thus, one can solve the Hamiltonian in the respective subspace using the ansatz $\Psi_{\pm}^{\dagger}\hat{H}_{\pm}\Psi_{\pm}$, where $|\Psi_{\pm}\rangle = |(\phi_{1\pm}\ \phi_{2\pm}\ \phi_{3\pm}\ \phi_{4\pm}\ \phi_{5\pm})\rangle$. The actual wave functions in the $\pm$ subspace will be given by $\psi_1 = \Sigma a_{i\pm}\phi_{i\pm}$, $\psi_2 = \Sigma b_{i\pm}\phi_{i\pm}$, $\psi_3 = \Sigma c_{i\pm}\phi_{i\pm}$, $\psi_4 = \Sigma d_{i\pm}\phi_{i\pm}$, and $\psi_5 = \Sigma e_{i\pm}\phi_{i\pm}$ where a_i, b_i, c_i, d_i, and e_i denote eigenfunctions of the $\hat{H}_{\pm}$ in the respective subspaces. Dipole moments can be calculated then between $\pm$ subspaces to study optical properties. Note that the configurations in the +ve subspace are connected by the current operator $\hat{j} \propto (itane/\hbar)\Sigma_l(c_{l+1}^{\dagger}c_l - c_l^{\dagger}c_{l+1})$ to the −ve subspace configurations, where a and e are lattice constant and electronic charge. On the other hand, configurations of the +ve subspace can be reached by operating the current operator twice on the ground state $|\phi_{1+}\rangle$. Results presented in the next section is for 12-site exact numerical solutions of Hamiltonian (1) based on the above-mentioned procedure.

III. CALCULATION OF LINEAR AND NONLINEAR OPTICAL SUSCEPTIBILITIES OF 1D MOTT INSULATORS

The electric field E of the incident light induces the dielectric polarization P_{ind} in a material, which is described by a power series of nonlinear optical susceptibility $\chi^{(n)}$: $P_{ind} = \epsilon_0\Sigma_{n=1,2,3,4,5,\ldots}(\chi^{(n)}E^n)$. The linear susceptibility $\chi^{(1)}$ is given by

$$\chi_{jk}^{(1)}(-\omega;\omega) = \frac{1}{\epsilon_0 N}\frac{e^2}{\hbar}\sum_b\left(\frac{\mu_{0b}^j\mu_{b0}^k}{E_b - i\Gamma_b - \omega} + \frac{\mu_{0b}^k\mu_{b0}^j}{E_b + i\Gamma_b + \omega}\right), \tag{2}$$

where N is the system size, ϵ_0 is the dielectric constant, j and k are the polarization directions, $e\mu_{0b}$ is the dipole moment between the ground state and the one-photon allowed odd-parity state, and E_b and Γ_b are energies of the one-photon states measured from the ground state and the damping factor, respectively. Due to prototype one-dimensional and centrosymmetric nature of Cu-O (Ni-X) network, the next higher-order optical susceptibilities $\chi^{(2)}$ will be vanishingly small in these systems. The third-order susceptibilities will be the lowest observable nonlinearities of interest and are expressed as[24]

$$\chi_{jklm}^{(3)}(-\omega_\sigma;\omega_1,\omega_2,\omega_3) = \frac{1}{\epsilon_0 N}\frac{e^4}{3!\hbar}P\sum_{a,b,c}\frac{\mu_{0b}^j\mu_{ba}^k\mu_{ac}^l\mu_{c0}^m}{(E_b - i\Gamma_b - \omega_\sigma)(E_a - i\Gamma_a - \omega_2 - \omega_3)(E_c - i\Gamma_c - \omega_3)}, \tag{3}$$

where $\omega_\sigma = \omega_1 + \omega_2 + \omega_3$, a and c denote even (two-photon allowed) and odd (one-photon allowed) states, respectively, and P represents permutations on the sums (j,ω_1), (k,ω_2), (l,ω_3), and (m,ω_σ). In the present study, $i=j=k=l=x$ is fixed, setting all the polarization directions the same along chains (Cu-O or Ni-X axis). The formal expression for the nonlinear susceptibility relevant to THG studies is obtained by considering $\omega_1 = \omega_2 = \omega_3 = \omega$ so that $\omega_\sigma = 3\omega$,

$$\chi^{(3)}_{THG}(-3\omega;\omega,\omega,\omega) = \frac{1}{\epsilon_0 N}\frac{e^4}{3!\hbar}\sum_{a,b,c}\frac{\mu^j_{0b}\mu^k_{ba}\mu^l_{ac}\mu^m_{c0}}{(E_b - i\Gamma_b - 3\omega)(E_a - i\Gamma_a - 2\omega)(E_c - i\Gamma_c - \omega)}. \quad (4)$$

Similarly, the formal expression for the nonlinear susceptibility relevant to TPA studies can be obtained by setting $\omega_1 = -\omega$ and $\omega_2 = \omega_3 = \omega$ as

$$\chi^{(3)}_{TPA}(-\omega;-\omega,\omega,\omega) = \frac{1}{\epsilon_0 N}\frac{e^4}{3!\hbar}\sum_{a,b,c}\frac{\mu^j_{0b}\mu^k_{ba}\mu^l_{ac}\mu^m_{c0}}{(E_b - i\Gamma_b - \omega)(E_a - i\Gamma_a - 2\omega)(E_c - i\Gamma_c - \omega)}. \quad (5)$$

We also study nonlinear susceptibility relevant to EA or dc Kerr effect by setting $\omega_1 = \omega_2 = 0$ and $\omega_3 = \omega$,

$$\chi^{(3)}_{EA}(-\omega;0,0,\omega) = \frac{1}{\epsilon_0 N}\frac{e^4}{3!\hbar}\sum_{a,b,c}\frac{\mu^j_{0b}\mu^k_{ba}\mu^l_{ac}\mu^m_{c0}}{(E_b - i\Gamma_b - \omega)(E_a - i\Gamma_a - \omega)(E_c - i\Gamma_c - \omega)}. \quad (6)$$

The triple sum in $\chi^{(3)}(-3\omega;\omega,\omega,\omega)$ is over all possible even- and odd-parity states and all the energies are with respect to the ground state. We calculated 300 excited states, 150 each for even- and odd-parity states of the model Hamiltonian (1), and compute $150\times150=22\,500$ dipole moments among them to evaluate various nonlinear optical properties such as THG, TPA, etc., through the above-mentioned formula. Before we talk about excited state nonlinearities, it is imperative to compare the available experimental data on THG, TPA, and EA with our theoretical calculation.

IV. RESULTS AND DISCUSSIONS

A. Ground state optics

In this section, our main aim is to provide conclusive evidence to the fact that there exists a higher-energy two-photon state in the THG than the two-photon state close to the first one-photon state. In order to observe such higher-energy two-photon state, one should evaluate $\mathrm{Im}\,\chi^{(3)}_{xxxx}(-\omega;\omega,-\omega,\omega)$ instead of $\mathrm{Im}\,\chi^{(3)}_{xxxx}(-\omega;0,0,\omega)$. Such a higher-energy two-photon state may also be observable in PA. Secondly, we would like to demonstrate that the observed intensity dependent refractive index (n_2) is well reproduced within our theoretical calculations. Thirdly, we show that the mechanism of huge optical nonlinearity is the same in all the so far observed 1D Mott-Hubbard insulator—it can be understood within large electron correlation, electronegativity of lattice ions, and chemical pressure.

In Fig. 1, a linear optical spectrum for various parameters is presented. The parameters are chosen to match experimental optical gap values. Positions of the optical gap should be compared with that of the two-photon state which are observable only in higher-order susceptibilities. The optical spectrum appears very similar to that obtained experimentally.[17] In order to achieve our first goal in this section, we study in detail the nature of the third-order susceptibility relevant for THG explicit expressions of which are given by Eq. (4). Parameters used in this section are $U_{\mathrm{Cu(Ni)}}=10.0$ eV, $U_{\mathrm{O}(X)}=6.0$ eV, $t_{\mathrm{Cu(Ni)\text{-}O}(X)}=1.0$ eV, $V=0.5$ eV, and $2\epsilon=1.0$ eV, unless specified otherwise. In Fig. 2, we have shown the nature of theoretically computed THG generation susceptibility expected from Hamiltonian (1) widely used for describing strongly correlated electron system. The imaginary part $\mathrm{Im}\,\chi^{(3)}_{xxxx}(-3\omega;\omega,\omega,\omega)$ [Fig. 2(a)], $\mathrm{Re}\,\chi^{(3)}_{xxxx}(-3\omega;\omega,\omega,\omega)$ [Fig. 1(b)], and the magnitude which was observed experimentally[15] $|\chi^{(3)}_{xxxx}(-3\omega;\omega,\omega,\omega)| = \sqrt{(\mathrm{Im}\,\chi^{(3)}_{xxxx})^2+(\mathrm{Re}\,\chi^{(3)}_{xxxx})^2}$ [Fig. 2(c)] are shown in Fig. 2 for comparison as a function of fundamental photon energy (in eV). It is evident in Figs. 2(a) and 2(b) that where the imaginary part (as a function of photon energy) rises the real part decreases and vice versa. This trend is also followed in Figs. 4 and 5. A look into Eq. (4) will lead to the fact that the THG susceptibility can have resonances at 3ω and 2ω corresponding to the three-photon resonant and two-photon resonant absorptions, respectively, as well as at ω for one-photon resonant absorptions. The nature of $|\chi^{(3)}_{xxxx}(-3\omega;\omega,\omega,\omega)|$ given in Fig. 2(c) is explainable given that the imaginary and real parts are displayed in Figs. 2(a) and 2(b). Very low intensity but broad absorption peak at ω_C is shown pronounced in the inset of Fig. 2(c). Given that nonlinearity in the lower-frequency regime is very large, the lower intensity peak at ω_C would still be observed experimentally if probed in the photon energy region as indicated in the inset of Fig. 2(c). We point out that the first peak at ω_A is a three-photon reso-

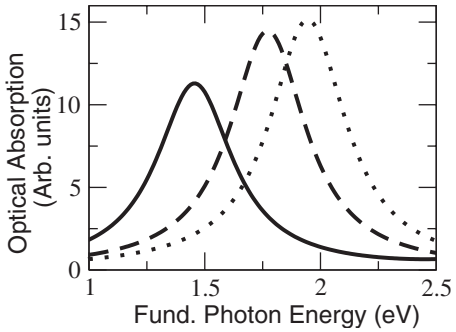

FIG. 1. Optical-absorption spectrum for one-dimensional Mott-Hubbard insulators with $U_{\mathrm{Cu(Ni)}}=10$ eV, $U_{\mathrm{O}(X)}=6$ eV. The spectrum denoted by the solid line corresponds to $V=\epsilon=0.5$ eV, $t=0.75$ eV, whereas the dashed and dotted lines correspond to $V=t=2\epsilon=1.0$ eV and $V=t=1.0$, $\epsilon=0.65$, respectively.

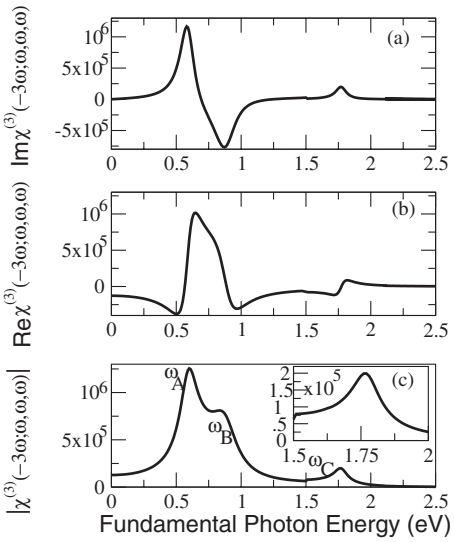

FIG. 2. Third-order susceptibility of one-dimensional Mott-Hubbard insulators relevant to third-harmonic generation. (a) Imaginary part of the THG susceptibility, (b) real part of the THG susceptibility, and (c) magnitude of the THG susceptibility. Locations of ω_A, ω_B, and ω_C are very close to the experimentally observed values. The peak at ω_A is a three-photon resonant absorption, whereas those at ω_B and ω_C are two-photon resonant absorptions.

nant one, whereas the peaks at ω_B and ω_C correspond to the lower- and higher-energy two-photon resonant absorptions, respectively. In order to identify two-photon resonant absorption peaks, we exhibit third-order susceptibilities relevant for two-photon absorption in Figs. 3 and 4.

In Fig. 3, we have plotted the imaginary and real parts of $\chi^{(3)}_{xxxx}(-\omega;-\omega,\omega,\omega)$, whereas in Fig. 4 the imaginary and real parts of $\chi^{(3)}_{xxxx}(-\omega;0,0,\omega)$. Im $\chi^{(3)}_{xxxx}(-\omega;-\omega,\omega,\omega)$ signifies two-photon absorption, whereas Re $\chi^{(3)}_{xxxx}(-\omega;-\omega,\omega,\omega)$ is related to the intensity dependent refractive index of a material. All-optical switching devices conventionally use the light-induced change of the refractive index n_2 rather than the two-photon absorption coefficient. Since the real and imaginary parts of the $\chi^{(3)}_{xxxx}(-\omega;-\omega,\omega,\omega)$ are related by Kramers-Kronig (KK) transformation, the observed strong TPA accompanied by large n_2 can be visualized from our theoretical calculations in Fig. 3. We would like to mention that only three experimental data points for n_2 are available,[9] but our theoretical results provide possible nature of n_2 as a function of the entire energy range. Our results on n_2 agree well with KK transformed observed TPA data, precisely indicating large values of n_2 near optical fiber communication wavelength (1.55 μm) that are also less dispersive (see, for example, the dashed curve). Concentrating toward Im $\chi^{(3)}_{xxxx}(-\omega;-\omega,\omega,\omega)$, the first peak is obviously a two-photon absorption which is exactly at the same photon energy as the second peak of Fig. 2(a). This conclusively proves that the second peak is a two-photon absorption, in agreement with the explanation of experimental observation.[15] In the same spirit, the third peak of Fig. 2(c) should be a two-photon resonant absorption which coincides with the dip of Fig. 3(a). In contrast, in Fig. 4(b) the dip of Im $\chi^{(3)}_{xxxx}(-\omega;0,0,\omega)$ is exactly at the double that of the second peak (ω_B) in Fig. 2(a), in accordance with the experimental observations [see, for example, Figs. 3(e), 3(f) of Ref. 15]. Thus, in order to observe the higher-energy two-photon state, one should measure the Im $\chi^{(3)}_{xxxx}(-\omega;-\omega,\omega,\omega)$, and a signature of the higher-energy peak is perhaps already there in the experimental observation [see, for example, Fig. 2(c) of Ref. 15].

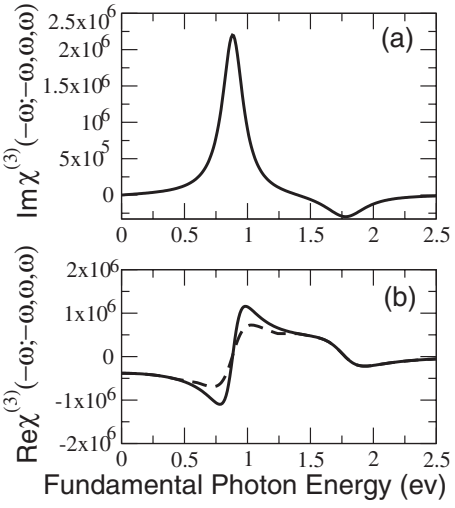

FIG. 3. Theoretical prediction of third-order susceptibility of one-dimensional Mott-Hubbard insulators relevant for two-photon absorption (TPA) as well as intensity dependent refractive index (n_2). Panel (a) represents the imaginary part of the third-order susceptibility, whereas (b) the real part. Both the real and imaginary parts show peaked structure around 0.88 eV (optical fiber communication length). The dashed curve in (b) corresponds to the case of higher value of linewidth parameter Γ_a=0.4 eV compared to the solid line case, Γ_a=0.3 eV.

Im $\chi^{(3)}_{xxxx}(-\omega,0,0,\omega)$ is related EA. A look to the expression in Eq. (6) indicates that it would show two-photon reso-

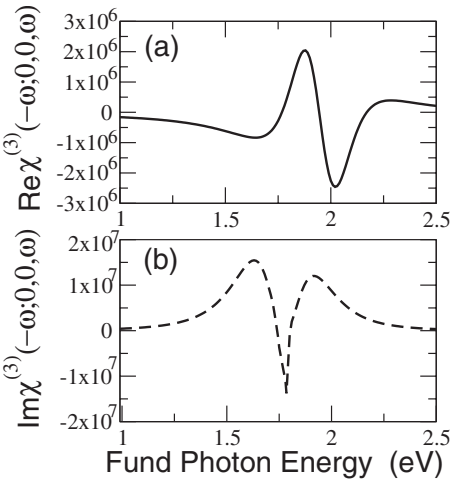

FIG. 4. Nature of (a) real and (b) imaginary parts of third-order susceptibility $\chi^{(3)}_{xxxx}(-\omega,0,0,\omega)$ in arbitrary units as a function of fundamental photon energy (in eV). Im $\chi^{(3)}_{xxxx}(-\omega,0,0,\omega)$ is related to electroabsorption (EA). The dip at around 1.77 eV in the EA spectra corresponds to the two-photon resonant peak seen at ω_B in the THG spectra.

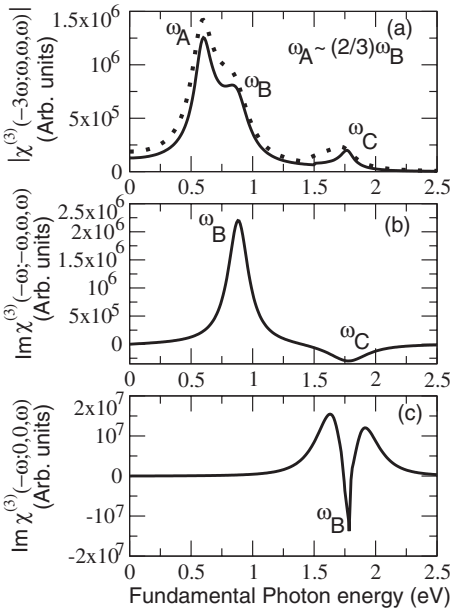

FIG. 5. Theoretical predictions of (a) THG, (b) TPA, and (c) EA. This figure conclusively proves that the third peak at ω_C is a two-photon resonant absorption which could be seen in the TPA spectra (b). The same should be observed in other one-dimensional Mott-Hubbard systems as well.

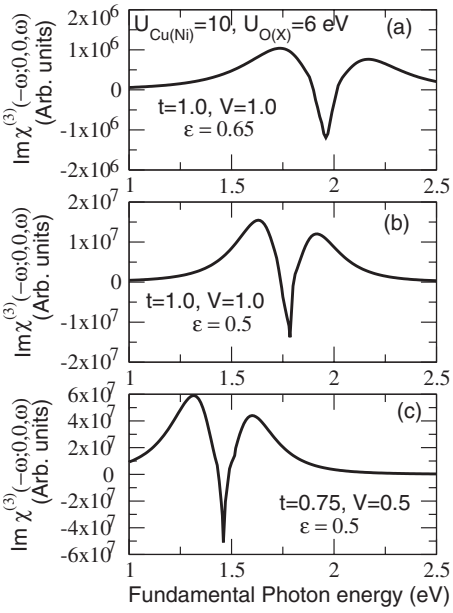

FIG. 6. Effect of lattice constant and charge-transfer energy in isostructural one-dimensional Mott-Hubbard insulators. For the same values of on-site Coulomb repulsions, in (a) ϵ=0.65, $V=t$ =1 eV; in (b) ϵ=0.5 eV, $V=t$=1 eV; and in (c) ϵ=0.5 eV=V, t =0.75 eV in order to simulate situation from Sr_2CuO_3 to $[Ni(chxn)_2Cl]Cl_2$ to $[Ni(chxn)_2Br]Br_2$.

nant states with resonance to ω. Thus, the dip in Fig. 4(b) actually corresponds to the second peak of Fig. 2(c). Im $\chi^{(3)}_{xxxx}(-\omega,0,0,\omega)$ thus possibly cannot probe such higher-energy peak at ω_C. Essence of all these results are summarized in Fig. 5 for convenience.

In Fig. 5(a), the magnitude of the THG susceptibility in arbitrary units is obtained as a function of fundamental photon energy. The first peak at ω_A corresponds to the three-photon resonant optical state, whereas the second peak at ω_B corresponds to the two-photon absorption peak which is slightly higher in energy than the optical state. There is a broad higher-energy two-photon resonant peak at ω_C, and as per the experimental findings[15] we exactly find $\omega_A \simeq 2\omega_B/3$ and $\omega_C \simeq 2\omega_B$ relationships. This is due to the fact that the two-photon resonant states appear at a frequency equal to half the fundamental frequency, whereas the three-photon resonant states at one-third that of fundamental frequency. Thus, the above relationship between ω_A and ω_B exists simply because of the fact that the first one- and two-photon states almost energetically degenerate. This does not hold in the case of Ca_2CuO_3 because the two-photon state is about 0.3 eV lower in energy than the one-photon state. This is precisely the reason why ω_{dip} does not coincide with ω_{peak} (see Fig. 4 of Ref. 15) in the case of Ca_2CuO_3. The dotted curve represents the same quantity for eight-site lattice size, indicating that there is marginal size effect.[25]

In Fig. 5(b), we plot the imaginary part of the third-order susceptibility, Im $\chi^{(3)}_{xxxx}(-\omega;\omega,-\omega,\omega)$, relevant for two-photon absorption. The broad peak at ω_B in Fig. 5(a) appears exactly at the first peak of Fig. 5(b). This conclusively proves that the peak at ω_B of Fig. 5(a) is the two-photon resonant state as it appears at the same wavelength in Fig. 5(b) too. Similarly, the broad peak at ω_C of Fig. 5(a) appears exactly at the dip frequency ω_c of Im $\chi^{(3)}_{xxxx}(-\omega;\omega,-\omega,\omega)$ shown in Fig. 5(b). Thus, the peak at ω_C of Fig. 5(a) is also a higher-energy two-photon resonant absorption.[15] We invite experimental measurements on Sr_2CuO_3, Ca_2CuO_3, Ni halide compounds of Im $\chi^{(3)}_{xxxx}(-\omega;\omega,-\omega,\omega)$ in order to verify the occurrence of higher-energy even-parity state.

Experimental studies on EA of one-dimensional Mott-Hubbard insulators are available in Refs. 3 and 15; while the former deals with Sr_2CuO_3 and Ca_2CuO_3 compounds, the latter deals with halogen-bridged Ni hallides, e.g., $[Ni(chxn)_2Cl]Cl_2$, $[Ni(chxn)_2Br]Br_2$, etc. In the case of cuprates,[3] only difference between the two isostructural compounds is the lattice constant which is smaller in the case of Ca_2CuO_3. This can lead to larger values of overlap between Cu-O ($t_{Cu\text{-}O}$) as well as intersite electron-electron repulsion (V). Considering the case of the two Ni hallide compounds mentioned above, they have difference in electronegativity of different hallides (Cl, Br) as well as difference in lattice constants.[26] Average bond distances Ni–X are different for different X ($d_{Ni\text{-}Cl} < d_{Ni\text{-}Br}$). Thus, the value of ϵ may be slightly larger in the case of Cl and so the value of $t_{Ni\text{-}Cl}$ compared to that for X=Br. The value of V should also modify accordingly (larger $d_{Ni\text{-}X}$, smaller V). In Fig. 6, we keep the values of on-site Coulomb repulsions fixed for all the three cases presented [(a)–(c)], whereas the values of t, V, and ϵ are as indicated in the respective figures. More than an order-of-magnitude enhancement in the values of $\chi^{(3)}_{EA}(-\omega;0,0,\omega)$ is found [from Fig. 6(a) to Fig. 6(c)]. There is also a reduction in the optical gap [from Fig. 6(a) to Fig. 6(c)] in accordance with the experimental observation [see, for example, Fig. 3 of Ref. 3]. We find that our results are in

TABLE I. The main contribution in $\chi^{(3)}_{EA}(-\omega;0,0,\omega)$ depends on the square of the product of dipole moments between the ground state to optical state (μ_{01}) and that between the optical state to the first two-photon state (μ_{12}). A correlation between the charge-transfer energy, electronic correlations, and nonlinearity is obtained. The optical gap (OG) is found to be less sensitive to values of $U_{\mathrm{Cu(Ni)}}$ or $U_{\mathrm{O}(X)}$ but more sensitive to the values of ϵ and t.

	$U_{\mathrm{Cu(Ni)}}=10.0$, $U_{\mathrm{O}(X)}=6.0$			
	$V=1$, $t=1$		$V=0.5$, $t=0.75$	
ϵ	OG	$\mu_{01}\mu_{12}$	OG	$\mu_{01}\mu_{12}$
0.25	1.41	88	1.08	181
0.50	1.77	864	1.45	1674
0.75	2.22	125	1.91	231
1.00	2.69	59	2.38	113
1.25	3.18	41	2.78	12

agreement with the already observed data. For example, the reduction in ϵ not only is sensitive to the optical gap but also enhances the nonlinearity [case of Figs. 6(a) and 6(b)]. In the case of bromide, the lattice constant is also larger compared to the chloride, which manifests in lower values of t as well as V. Although we have kept value of ϵ fixed in Figs. 6(b) and 6(c), the optical gap is reduced further to around 1.4 eV. It is conceivable that slightly lowering the value of ϵ will reproduce the experimental optical gap of 1.32 eV. We have not changed the value of ϵ in Figs. 6(b) and 6(c) purposefully because the effect of change in ϵ is already understood in Figs 6(a) and 6(b) and the effect of t is to be understood. We notice that the optical gap is more sensitive to the value of t than to ϵ because the charge-transfer energy E_{CT} is given by $E_{CT}=\epsilon+\sqrt{\epsilon^2+2t^2}$. A close look to the Tables I and II would indicate that the optical gap is insensitive to the values of U's. In correlated systems like this, values of t get renormalized[27] by electron correlation, and if one uses the renormalized values of t, the optical gaps obtained through exact diagonalization are reproducible via the above-mentioned formula of E_{CT}. We would further like to mention that the same values of U and V are found to fit the valence-band photoemission spectra of both the Sr_2CuO_3 and Ca_2CuO_3 compounds, except the charge-transfer energy—a reduced value of charge-transfer energy in the case of Sr_2CuO_3.[28] This also clearly suggests lower value of t in the case of Sr_2CuO_3. A further explanation to such large nonlinearity may also be understood as follows. The main term dominating the spectral shape of $\chi^{(3)}_{xxxx}(-\omega;0,0,\omega)$ may be expressed as

$$\chi^{(3)}_{xxxx}(-\omega;0,0,\omega) \propto \frac{\mu_{01}\mu_{12}\mu_{21}\mu_{10}}{(E_1-i\Gamma_b-\omega)(E_2-i\Gamma_a-\omega)(E_1-i\Gamma_b-\omega)}. \quad (7)$$

Here, indices 0, 1, and 2 represent, respectively, the ground, one-photon allowed, and two-photon allowed states. In Tables I and II, we thus tabulate the optical gap (OG) and the product $\mu_{01}\mu_{12}$ for various parameters. With the discussions above and detailed tables, we believe that the mechanism of optical nonlinearities is the same in all the discussed 1D Mott-Hubbard insulators and can be understood within the extended Hubbard model. Furthermore, the linewidth parameters play a strong role too, which is smallest in the case of Ni-Br compounds and largest in the case Ca_2CuO_3. In particular, maximum values of $\mathrm{Im}|\chi^{(3)}(-\omega;0,0,\omega)|$ range from 10^{-5} to 10^{-8} esu as found in reality.

In the strong correlation limit, the ground state comprises a state that contains each Cu site occupied in antiferromagnetic fashion. The lowest possible excitations occur when the Cu spin moves to the left or/and right neighboring O. The lowest one-photon and two-photon states comprise the odd $(-)$ and even $(+)$ combinations of the above-mentioned excitations which are called as odd and even charge-transfer (CT) states, respectively. Due to strongly correlated nature of wave functions, both these states are energetically almost degenerate and this can cause very strong dipole coupling between these even and odd CT states. We will come back to this point again later and show that this is the cause of gigantic enhancement in excited state nonlinearity in these classes of materials. There are higher-energy excitations in which two and/or three of the Cu spins move to its neighboring O. Also, there are excitations wherein one of the Cu spin moves to its neighboring O together with the neighboring Cu spin occupying the earlier Cu (spin of which moved to the neighboring O). The eigenstate of the higher-energy two-photon state seen at ω_C is quite complicated but is an *even and almost equal* combination of all the excitations mentioned above. The photoexcitation process in band insulators creates an electron-hole pair bound by their attractive Coulomb interaction (Mott-Wannier exciton). The pair gives a series of bound states with odd and even parities below the gap. This is the case of silicon polymers and Pt halides, where the odd- and even-parity excited states are separated by an energy gap as large as 1 eV, which is unfavorable for large dipole moment (as it is inversely proportional to the energy difference between the pairs of states). In contrast, one-dimensional undoped Mott-Hubbard insulators are one hole per (Cu/Ni) site in which the ground state is antiferro-

TABLE II. Same as Table I but for different values of on-site electronic correlations. For larger values of on-site electronic correlations, maximum nonlinearity shifts toward lower values of optical gap.

	$U_{\mathrm{Cu(Ni)}}=12.0$, $U_{\mathrm{O}(X)}=6.0$			
	$V=1$, $t=1$		$V=0.5$, $t=0.75$	
ϵ	OG	$\mu_{01}\mu_{12}$	OG	$\mu_{01}\mu_{12}$
0.25	1.42	142	1.08	273
0.35	1.55	260	1.22	2975
0.40	1.63	200	1.31	734
0.43	1.68	3178	1.35	412
0.45	1.72	731	1.39	317
0.5	1.81	246	1.47	197
0.75	2.26	51	1.93	59

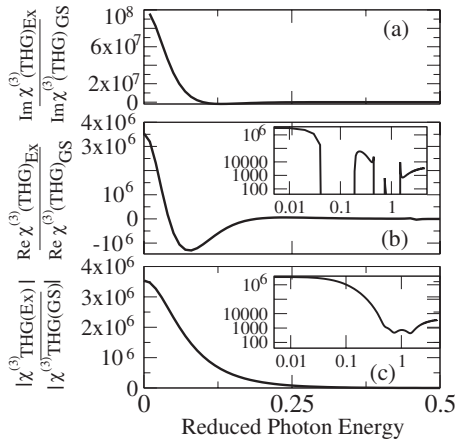

FIG. 7. Theoretical prediction of enhanced excited state nonlinearity in one-dimensional Mott insulators. Panel (a) represents the ratio of the imaginary part of the THG susceptibility from the two-photon allowed state to that from the ground state. The latter is the same as that presented in Fig. 1(a). Panel (b) represents the ratio of the real part of the THG evaluated from the excited state to the ground state. Panel (c) represents the ratio of the magnitudes of the THG as indicated in the axis labels. The inset figures are indicative of the same as that of the main figure but in logarithmic scale.

magnetically ordered. In the charge excitation, the Cu hole can move to either of its left and right O, odd $(-)$ and even $(+)$ combination of which forms the optical state and the first two-photon state, respectively. Due to strong electron correlations present in these systems, the odd- and even-parity charge-transfer states are nearly energetically degenerate and have strong dipole moment. [Also, the Cu spin can move back to it from the O with its spin flipped, giving rise to spin excitation or "spinon" which is gapless and arises close in energy to the ground state; this is optically silent (see, for example, Ref. 29).] Thus, the combined effect of confinement (one dimensionality) and strong Coulomb repulsion along with charge transfer is responsible for the huge optical nonlinearity in low-dimensional Mott-Hubbard insulators. In two dimensions, one thus expects $--,++$, $-+,+-$ symmetries since the Cu hole can also move to up and down oxygen. $++$ has the same symmetry as the ground state. $+-$ and $-+$ are degenerate and are the optical states. The dipole coupling between the one-photon $(+-$ and $-+)$ and two-photon $(++)$ states then involves only two of the four configurations. Therefore, the transition dipole moments between the ground and one-photon states as well as between one-photon and two-photon states are expected to be weaker than that for the 1D case and hence the nonlinearities. Thus, we confined our discussions only to one-dimensional systems.

B. Excited state nonlinear optics

So far, we discussed about the ground state optical nonlinear, e.g., THG, TPA, and EA, processes and compared our theoretical evaluations with available experimental data. In Fig. 7, gigantic enhancement in various third-order optical susceptibilities from the first two-photon allowed state (and hence excited state nonlinearities) in comparison to that from the ground state is presented. It should be noted that the ground state optical nonlinearities in one-dimensional strongly correlated systems are already quite large[2,3,9,15] compared to other low-dimensional materials. Therefore, enhancement in excited state nonlinearities of the order of 8 orders of magnitude is really remarkable. We present below a theoretical enhancement mechanism for third-order nonlinear processes originating from real population of electronic excited states in strongly correlated systems. In experiments, an electronic excited state (the lowest two-photon state in the present case) can be generated by using laser pulse at certain wavelength and then populated for time long enough to permit nonresonant measurements. Principal reasons for the enhancement of the nonlinearity from the excited state are as follows. The transition energy between the first optical state and the two-photon $(2A_g)$ state is the smallest, whereas the dipole moment between them is the strongest. Physical reason for the same is discussed in the earlier section. Here, we would like to comment on the fact that the experimental determination of the energy difference between one- and two-photon states could be even smaller. This is because of the following reasons. We have provided ample evidences from theoretical as well as experimental studies[3] that the dip in Im $\chi^{(3)}_{xxxx}(-\omega;0,0,\omega)$ corresponds to the location of two-photon state, whereas experimentally (see Fig 3. of Ref. 3 and Fig. 9 of Ref. 17) it is indicated quite away from the same. Thus, the energy difference between one- and two-photon states could be even smaller and energy ordering could even be reversed in accordance with Ref. 15. It is to be noted that in their three-level approximation, the one-photon state is always taken below the two-photon state. Although in the case of cuprates they locate the two-photon state below the one-photon state, the reverse is true for the Ni halides. The ratio of the dipole moments between the optical state to the first two-photon state in comparison to that from the ground state to the optical state is an order of magnitude larger. The value of the ratio can go from 50 to 500 (see also Tables I and II) in our calculation depending on various combinations of the parameters. For example, a combination of the parameters ($|t|=1.0$ eV, $U_{\mathrm{Cu(Ni)}}=10$ eV, $U_{\mathrm{O}(X)}=6$ eV, $V=1.0$ eV, a relatively large value of linewidth parameter $\Gamma=0.2$ eV) is such that the ratio is around 50. This property of the above-mentioned one-dimensional strongly correlated electron system is also seen experimentally (see, for example, Fig. 5(b) of Ref. 3). As we mentioned earlier, due to strongly correlated nature of electronic states the odd and even CT states which are the first excited one- and two-photon states are almost energetically degenerate and contribute to extremely large dipole coupling between them. If one exchanges over the positions of odd- and even-parity states in Eqs. (3)–(5), numerators of the optical excited state nonlinear susceptibility for THG, TPA, and EA can be obtained. Since this is a nonresonant process, the denominator may not play significant role (except at very low frequency). The maximum contribution comes from $a=c=2$ and $b=1$ terms of the triple sums. Furthermore, the ground state 0 should be replaced by $a=2$. As a result, first optical state nonlinearity can be enhanced as large as $(50)^4$ compared to

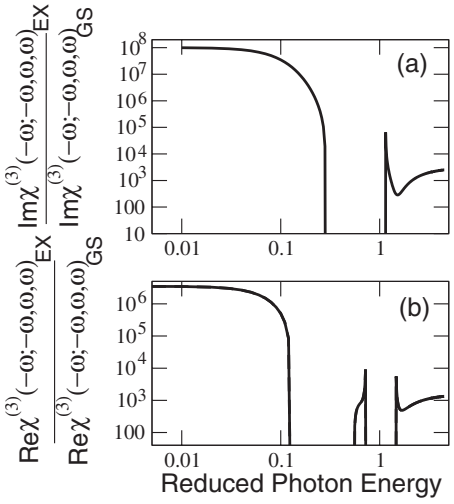

FIG. 8. Excited state enhancement of (a) imaginary and (b) real parts of the third-order susceptibility with respect to the ground state relevant for TPA in logarithmic scale.

that from the ground state. This is reflected in Figs. 7–9. While Fig. 7 deals with excited state THG susceptibilities (magnitude, real and imaginary parts), Figs. 8 and 9 deal with excited state TPA and EA susceptibilities respectively. In Fig. 7 the inset figures are in logarithmic scale, which is the same for Figs. 8 and 9. 6–8 orders of magnitude enhancement in the terahertz frequency region and about 3 orders of magnitude enhancement in the optical fiber communication wavelength are theoretically predicted.

In general, transition energies of $\hbar\omega_{bS_1}$ between the spin state S_1 and intermediate virtual one photon b ($b<150$ in our study) states are all smaller than the transition energies of the S_0 ground state excitation processes. Furthermore, many excited states with large transition dipole moments are accessible through the populated S_1 state and the S_b excited states. It is understandable that the smaller transition energies $\hbar\omega_{ba}$ and larger transition dipole moment of μ_{ab} cause individual excitation process that makes up $\chi^{(3)}$ at the S_1 state to be

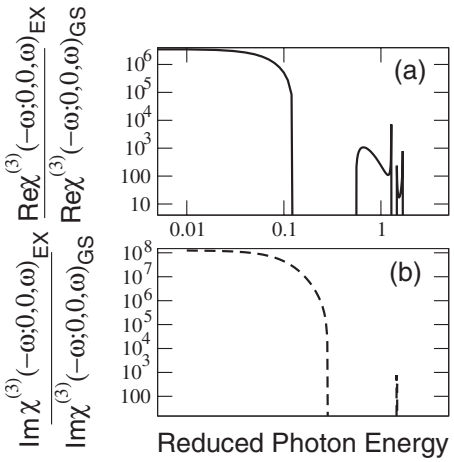

FIG. 9. Excited state enhancement of (a) real and (b) imaginary parts of the third-order susceptibility with respect to the ground state relevant for EA in logarithmic scale.

larger than those of $\chi^{(3)}$ at the ground state S_0. In addition, there are two different channels that contribute to the $\chi^{(3)}$. Channel 1: $S_0 \rightarrow S_b \rightarrow S_0 \rightarrow S_b \rightarrow S_0$, where S_b is a one-photon allowed excited state. This process can make negative contribution to $\chi^{(3)}$. Channel 2: $S_0 \rightarrow S_b \rightarrow S_a \rightarrow S_b \rightarrow S_0$, where S_a is a two-photon allowed excited state. In contrast to $\chi^{(3)}$ at S_0 which is dominantly channel 1 process, $\chi^{(3)}$ at S_1 is composed of a large number of terms that not only are individually larger than those of $\chi^{(3)}$ at S_0 but also have a reduced degree of cancellation effect (i.e., having same sign between channel 1 and 2 processes).

C. Phenyl based π-conjugated polymer

In this section, our primary motivation is to provide explicit calculation of excited state optical nonlinearity of one of the organic systems, namely, poly-(paraphenylenevenylene) (PPV), for direct comparison to one-dimensional Mott-Hubbard systems. We study various oligomers of PPV (PPV_n, $n=3,4,\ldots,7$) within a rigid-band correlated π-electron model such as the Pariser-Parr-Pople model Hamiltonian,[30]

$$H = -\sum_{\langle ij\rangle,\sigma} t_{ij}(c_{i\sigma}^{\dagger}c_{j\sigma} + c_{j\sigma}^{\dagger}c_{i\sigma}) + U\sum_{i} n_{i\uparrow}n_{i\downarrow} + \sum_{i<j} V_{ij}(n_i - 1)(n_j - 1), \tag{8}$$

where $\langle ij\rangle$ implies nearest neighbors, $c_{i\sigma}^{\dagger}$ creates an electron of spin σ on the p_z orbital of carbon atom i, $n_{i\sigma}=c_{i\sigma}^{\dagger}c_{i\sigma}$ is the number of electrons with spin σ, and $n_i=\Sigma_\sigma n_{i\sigma}$ is the total number of electrons on atom i. The parameters U and V_{ij} are the on-site and long-range Coulomb repulsions, respectively, while t_{ij} is the nearest-neighbor one-electron hopping matrix element that includes bond alternation and connectivity. The bond alternation appears due to electron-phonon interaction when treated in SSH[31] fashion. The parametrization of the intersite Coulomb interactions is done in a manner similar to the Ohno parametrization,[32]

$$V_{i,j} = U/\kappa(1 + 0.6117R_{i,j}^2)^{1/2}, \tag{9}$$

where κ is a parameter which has been introduced to account for the possible screening of the Coulomb interactions in the system.[33–35] We have examined both the standard Ohno parameters ($U=11.13$ eV, $\kappa=1.0$) as well as a particular combination of U and κ ($U=8.0$ eV, $\kappa=2.0$) that was found previously to be satisfactory at a semiquantitative level for explaining the full wavelength dependent ground state absorption spectrum of PPV;[33,34,36] the latter set of values is used here, more so because the former set does not reproduce the observed PA data. We took $t=-2.4$ eV for the C-C bond in benzene rings and -2.2 eV for the vinylene linkage of the PPV oligomer single bond and -2.6 eV for the double bond. We considered PPV oligomers in their planar configurations, with the conjugation direction along the x axis. Thus, the symmetry group of PPV oligomers is C_{2h}. The two-photon states of the PPV oligomers belong to the A_g irreducible representation (irrep) of the respective symmetry group, while the one-photon states belong to the B_u irrep. The

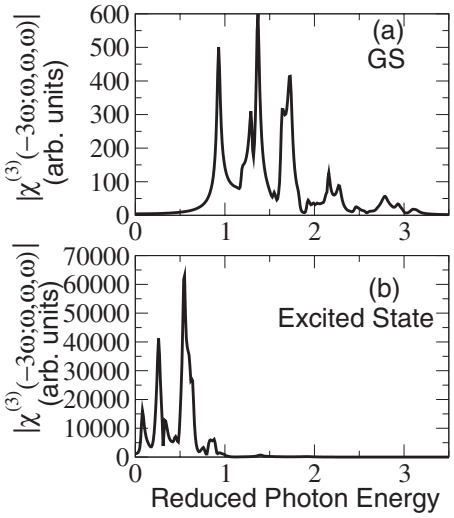

FIG. 10. (a) Third-harmonic generation (THG) susceptibility and (b) excited state THG susceptibility for poly-(paraphenylenevenylene) (PPV).

many-body correlated electron calculations were achieved using the multireference singles and doubles configuration-interaction approach, which is a powerful configuration-interaction technique[37] that has been used previously for linear-chain polyenes by Tavan and Schulten[38] as well as others,[39] and by us to calculate the excited state ordering in polyphenyl- and polydiphenylacetylenes.[40] We calculate 100 excited states including the ground state, i.e., 50 in each subspace (A_g and B_u), and subsequently $50\times 50=2500$ transition dipole moments between them for each oligomer of PPV are obtained to calculate various nonlinear optical properties. Given that dimensions of Hamiltonian matrices are naturally rather large (of the order of several millions) together with large numbers of dipole-moment calculations, the method is highly accurate although extremely tedious and time and space expensive.

In Fig. 10, we show the results of (a) ground state and (b) excited state THG susceptibility for PPV oligomer (6 units). There is more than 2 orders of magnitude enhancement in the excited state THG susceptibility. The enhancement magnitude does not change much with larger oligomer lengths. The ground state THG susceptibility shown in Fig. 10(a) qualitatively agrees well with observed data.[40] We would like to further mention that similar calculations for π-conjugated polymers such as trans-polyacetylene have also been performed through highly accurate quantum chemistry method called multireference single double configuration interaction[41,42] and one can expect excited state (optical) nonlinearity by about 2 orders of magnitude in comparison to that from the ground state (details of which would be reported elsewhere). Thus, superiority of one-dimensional Mott-Hubbard insulators over π-conjugated organic materials as far as excited state nonlinearities are concerned is established.

V. SUMMARY AND CONCLUSIONS

The realization of all-optical switching, modulating and computing devices is an important goal in modern optical technology. Nonlinear optical materials with large third-order nonlinear susceptibilities, fast response time, low loss, and operability at room temperature are indispensable for such devices, because the magnitudes of these quantities strongly influence the instrument performance. Large optical nonlinearity and subpicosecond recovery are known in organic materials[43,44] but further improvement in sample quality and morphology is required for actual application. The strongly correlated one-dimensional Mott insulators such as Sr_2CuO_3 and Ca_2CuO_3 on the one hand posseses large nonlinearity, ultrafast recovery time comparable to organics, superior thermal conductivity, and higher damage threshold of inorganic.[2,9] This along with such a huge enhancement in the excited state nonlinearity would perhaps make these materials appropriate for all-optical switch devices. Until recently, the terahertz (1 THz$=10^{12}$ Hz) region of the electromagnetic spectrum from about 100 GHz to 10 THz has been almost inaccessible because of the lack of efficient sources and detectors in this terahertz gap. A detailed discussion of the terahertz sources, coherent detectors, and modulators is given in Ref. 45. Terahertz communication is in the very early stages of development, with first data transmission in this frequency range recently reported.[46] The terahertz regime is 1 THz $=33.3$ cm^{-1} (wave number)$=300$ μm (wavelength)$=4.1$ meV (in comparison, optical fiber communication wavelength is 1.55 μm$=0.8$ eV). In Figs. 7–9, we have shown the excited state enhancement in nonlinearities in the lower-frequency regime (longer wavelength) relevant for terahertz and intermediate frequency regime and optical fiber communications regime, respectively. It is evident from the Figs. 7–9 that in the terahertz communication region, the optical nonlinearity is several orders of magnitude larger, *which may not be possible to achieve* from ground state. Therefore, we hope that the one-dimensional strongly correlated systems such as Sr_2CuO_3, Ca_2CuO_3, etc., may be usable as nonlinear optical medium suitable for terahertz communication by actually populating the first two-photon state at a sufficiently long enough time such that the system can be operated for nonresonant nonlinear process.

We have discussed in detail the origin of giant ground and excited nonlinear optical properties in low-dimensional Mott-Hubbard insulators. We have theoretically demonstrated the observed THG spectrum and that the *oscillatory structure* at ω_C is another-higher energy two-photon state which may be verified experimentally. We also presented TPA and EA theoretically and compare with available experimental data. These results of ground state nonlinear as well as linear properties compare well with experiments. Then, we considered the case of third-order nonlinear optical susceptibilities from an excited state rather than the ground state. We predict from our theoretical calculation that these classes of materials would have *several orders of magnitude larger* excited state optical nonlinearities (e.g., excited state THG, TPA, EA) compared to that from the ground state in the terahertz frequency regime. Theoretically (as well as from already known experimental data), we emphasize that this is an artifact of strongly correlated nature of these systems—π-conjugated polymers can also have about 2 orders of magnitude larger excited state optical nonlinearity compared to that of the ground state. So far, it is well known

that π-conjugated organic molecules and polymer systems are of interest due to the delocalized π-electron systems which give rise to large values of $\chi^{(3)}$, but one-dimensional Mott-Hubbard systems, on the contrary, are not so delocalized but dominated by electron-electron repulsion. We pointed out discrepancies in earlier experimental studies as far as energy orderings of lowest one- and two-photon states are concerned. We pointed out its immense significance as far as excited state nonlinearities are concerned. For example, one can populate the optical state with appropriate excitation which would be depopulated to the lowest two-photon state at ultrashort time and would stay there for sufficient time because it is dipolly forbidden to the ground state. (This seems to be the actual case for cuprates.[17]) Also, excited state nonlinearity dependence on the degree of population of the concerned excited state is shown. Since the two electronic one- and two-photon states are energetically degenerate, direct jump from the one-photon state to the lower two-photon state may be expected from the cuprates, which *would* emit terahertz radiations. Thus, cuprates could be a great terahertz radiation source, which must be experimentally verified. For a case study of Ca_2CuO_3, negative photoinduced absorption (PA) was predicted.[29] Furthermore, choice of large optical nonlinear medium depends not only on the ground state but also on the excited state matter.[19]

Finally, we have studied and solved finite-size[25] one-dimensional extended Hubbard model exactly to model one-dimensional strongly correlated systems. We showed that the calculated THG spectrum reproduces exceptionally well the experimentally observed one. We pointed out that there exists a higher-energy two-photon state which can be experimentally verified. Most importantly, we showed that these materials would be a potential candidate for next generation on chip terahertz communication for which excited state nonlinearity is essential. This is because of the *unique* strongly correlated nature of these systems which makes the lowest CT one-photon and two-photon states almost energetically overlapping and very large dipole coupling between them. Like electron-electron correlation has modified many fundamental notions of superconductivity (e.g., high-T_c superconductivity compared to BCS), magnetism (compared to band magnetism), and metal-insulator transition, application of these materials for on chip terahertz communication and all-optical switching devices would perhaps bring a different era in optics too.

ACKNOWLEDGMENTS

The author thanks S. C. Mehendale, S. Mazumdar, and A. Shukla for useful discussions and Rama Chari for useful discussions and comments on terahertz on chip communications. The author also thanks Max Planck Institute for Complex Systems, Dresden, Germany for financial support.

*Electronic address: hng@mpipks-dresden.mpg.de

[1] P. W. Anderson, Nature (London) **235**, 1196 (1987); S. R. Julian, C. Pfleiderer, F. M. Grosche, N. D. Mathur, G. J. McMullan, A. J. Diver, I. R. Walker, and G. G. Lonzarich, J. Phys.: Condens. Matter **8**, 9675 (1996).

[2] T. Ogasawara, M. Ashida, N. Motoyama, H. Eisaki, S. Uchida, Y. Tokura, H. Ghosh, A. Shukla, S. Mazumdar, and M. Kuwata-Gonokami, Phys. Rev. Lett. **85**, 2204 (2000).

[3] H. Kishida, H. Matsuzaki, H. Okamoto, T. Manabe, M. Yamashita, Y. Taguchi, and Y. Tokura, Nature (London) **405**, 929 (2000).

[4] Y. Mizuno, K. Tsutsui, T. Tohyama, and S. Maekawa, Phys. Rev. B **62**, R4769 (2000).

[5] G. P. Zhang, Phys. Rev. Lett. **86**, 2086 (2001).

[6] C. Kim, J. Electron Spectrosc. Relat. Phenom. **117**, 503 (2001); Sadamichi Maekawa and Takami Tohyama, Rep. Prog. Phys. **64**, 383 (2001).

[7] Akira Takahashi, Hiroki Gomi, and Masaki Aihara, Phys. Rev. B **69**, 075116 (2004).

[8] I. A. Zaliznyak, H. Woo, T. G. Perring, C. L. Broholm, C. D. Frost, and H. Takagi, Phys. Rev. Lett. **93**, 087202 (2004).

[9] M. Ashida, T. Ogasawara, Y. Tokura, S. Uchida, S. Mazumdar, and M. Kuwata-Gonokami, Appl. Phys. Lett. **78**, 2831 (2001).

[10] S. Iwai, M. Ono, A. Maeda, H. Matsuzaki, H. Kishida, H. Okamoto, and Y. Tokura, Phys. Rev. Lett. **91**, 057401 (2003).

[11] A. S. Moskvin, J. Málek, M. Knupfer, R. Neudert, J. Fink, R. Hayn, S.-L. Drechsler, N. Motoyama, H. Eisaki, and S. Uchida, Phys. Rev. Lett. **91**, 037001 (2003).

[12] M. Ashida, T. Ogasawara, N. Motoyama, H. Eisaki, S. Uchida, Y. Taguchi, Y. Tokura, M. Kuwata-Gonokami, H. Ghosh, A. Shukla, and S. Mazumdar, Int. J. Mod. Phys. B **15**, 3628 (2001); Proceedings of the International Conference on Excitonic Processes in Condensed Matter EXCON 2000, 2000 (unpublished), p. 60.

[13] Makoto Takahashi, Takami Tohyama, and Sadamichi Maekawa, Phys. Rev. B **66**, 125102 (2002); M. Ashida, Y. Taguchi, Y. Tokura, R. T. Clay, S. Mazumdar, Yu. P. Svirko, and M. Kuwata-Gonokami, Europhys. Lett. **58**, 455 (2002).

[14] A. Schülzgen, Y. Kawabe, E. Hanamura, A. Yamanaka, P.-A. Blanche, J. Lee, H. Sato, M. Naito, N. T. Dan, S. Uchida, Y. Tanabe, and N. Peyghambarian, Phys. Rev. Lett. **86**, 3164 (2001). For femtosecond studies, see K. Matsuda, I. Hirabayashi, K. Kawamoto, T. Nabatame, T. Tokizaki, and A. Nakamura, Phys. Rev. B **50**, 4097 (1994); K. Matsuda, Physica C **280**, 84 (1997); R. A. Kaindl, M. Woerner, T. Elsaesser, D. C. Smith, J. F. Ryan, G. Farnan, M. McCurry, and G. Walmsley, Science **287**, 470 (2000); Physica C **341–348**, 2213 (2000). For magnetic excitations, see J. D. Perkins, J. M. Graybeal, M. A. Kastner, R. J. Birgeneau, J. P. Falck, and M. Greven, Phys. Rev. Lett. **71**, 1621 (1993); J. Lorenzana and G. A. Sawatzky, *ibid.* **74**, 1867 (1995); N. Motoyama, H. Eisaki, and S. Uchida, *ibid.* **76**, 3212 (1996); H. Suzuura, H. Yasuhara, A. Furusaki, N. Nagaosa, and Y. Tokura, *ibid.* **76**, 2579 (1996).

[15] H. Kishida, M. Ono, K. Miura, H. Okamoto, M. Izumi, T. Manako, M. Kawasaki, Y. Taguchi, Y. Tokura, T. Tohyama, K. Tsutsui, and S. Maekawa, Phys. Rev. Lett. **87**, 177401 (2001).

[16] A. Maeda, M. Ono, H. Kishida, T. Manako, A. Sawa, M. Kawasaki, Y. Tokura, and H. Okamoto, Phys. Rev. B **70**, 125117 (2004).

[17] M. Ono, K. Miura, A. Maeda, H. Matsuzaki, H. Kishida, Y. Taguchi, Y. Tokura, M. Yamashita, and H. Okamoto, Phys. Rev. B **70**, 085101 (2004).

[18] Q. L. Zhou, J. R. Heflin, K. Y. Wong, O. Zamani-Khamiri, and A. F. Garito, Phys. Rev. A **43**, 1673 (1991); D. C. Rodenberger, J. R. Heflin, and A. F. Garito, Nature (London) **359**, 309 (1992); J. R. Heflin, D. C. Rodenberger, R. F. Shi, M. Wu, N. Q. Wang, Y. M. Cai, and A. F. Garito, Phys. Rev. A **45**, R4233 (1992); D. C. Rodenberger, J. R. Heflin, and A. F. Garito, *ibid.* **51**, 3234 (1995).

[19] S. R. Marder, J. W. Perry, G. Bourhill, C. B. Gorman, B. G. Tiemann, and K. Mansour, Science **261**, 186 (1993); S. R. Marder, L.-T. Cheng, B. G. Tiemann, A. C. Friedli, M. Blanchard-Desce, J. W. Perry, and J. Skindhoj, *ibid.* **263**, 511 (1994); S. R. Marder, C. B. Gorman, F. Meyers, J. W. Perry, G. Bourhill, J.-L. Bredas, and B. M. Pierce, *ibid.* **265**, 632 (1994); S. R. Marder, W. E. Torruellas, M. Blanchard-Desce, V. Ricci, G. I. Stegeman, S. Gilmour, J.-L. Brèdas, J. Li, G. Bublitz, and S. G. Boxer, *ibid.* **276**, 1233 (1997).

[20] Lin X. Chen and D. Philip Laibale, Chem. Phys. Lett. **270**, 255 (1997).

[21] Masatoshi Yamada, Atsushi Fujimori, and Yoshinori Tokura, Rev. Mod. Phys. **70**, 1039 (1998).

[22] S. Mazumdar and Z. Soos, Synth. Met. **1**, 77 (1979); S. N. Dixit and S. Mazumdar, Phys. Rev. B **29**, 1824 (1984).

[23] S. Ramasesha and Krishna Das, Phys. Rev. B **42**, 10682 (1990); Bhabadyuti Sinha and S. Ramasesha, *ibid.* **48**, 16410 (1993); E. Tekman and S. Ciraci, *ibid.* **42**, 9098 (1990).

[24] P. N. Butcher and D. Cotter, *The Elements of Nonlinear Optics* (Cambridge University Press, Cambridge, 1990).

[25] Finite-size effects in optical conductivity based on Hubbard model are discussed by C. A. Stafford, A. J. Millis, and B. S. Shastry, Phys. Rev. B **43**, 13660 (1991). Size effects are already negligible for $N>12$. Moreover, excited state nonlinearities were presented in terms of ratios (excited state to the ground state).

[26] H. Okamoto, Y. Shimada, Y. Oka, A. Chainani, T. Takahashi, H. Kitagawa, T. Mitani, K. Toriumi, K. Inoue, T. Manabe, and M. Yamashita, Phys. Rev. B **54**, 8438 (1996).

[27] M. Mitra, Haranath Ghosh, and S. N. Behera, Eur. Phys. J. B **2**, 371 (1998).

[28] K. Maiti, D. D. Sarma, T. Mizokawa, and A. Fujimori, Phys. Rev. B **57**, 1572 (1998).

[29] Haranath Ghosh, Europhys. Lett. **75**, 468 (2006).

[30] R. Pariser and R. G. Parr, J. Chem. Phys. **21**, 466 (1953); J. A. Pople, Trans. Faraday Soc. **49**, 1375 (1953).

[31] A. J. Heeger, S. Kivelson, J. R. Schrieffer, and W.-P. Su, Rev. Mod. Phys. **60**, 781 (1988).

[32] K. Ohno, Theor. Chim. Acta **2**, 219 (1964).

[33] M. Chandross, S. Mazumdar, M. Liess, P. A. Lane, Z. V. Vardeny, M. Hamaguchi, and K. Yoshino, Phys. Rev. B **55**, 1486 (1997).

[34] M. Chandross, S. Mazumdar, S. Jeglinski, X. Wei, Z. V. Vardeny, E. W. Kwock, and T. M. Miller, Phys. Rev. B **50**, 14702 (1994).

[35] C. W. M. Castleton and W. Barford, J. Chem. Phys. **117**, 3570 (2002).

[36] D. Guo, S. Mazumdar, S. N. Dixit, F. Kajzar, F. Jarka, Y. Kawabe, and N. Peyghambarian, Phys. Rev. B **48**, 1433 (1993).

[37] R. J. Buenker and S. D. Peyerimhoff, Theor. Chim. Acta **35**, 33 (1974).

[38] P. Tavan and K. Schulten, Phys. Rev. B **36**, 4337 (1987).

[39] D. Beljonne, Habilitation thesis, Université de Mons-Hainaut, Belgium, 2001.

[40] Haranath Ghosh, Chem. Phys. Lett. **426**, 431 (2006).

[41] Haranath Ghosh, A. Shukla, and S. Mazumdar, Phys. Rev. B **62**, 12763 (2000).

[42] A. Shukla, Haranath Ghosh, and S. Mazumdar, Phys. Rev. B **67**, 245203 (2003).

[43] *Nonlinear Optical Properties of Organic Molecules and Crystals*, edited by D. S. Chemla and J. Zyss (Academic, Orlando, 1987).

[44] *Nonlinear Optical Effects in Organic Polymers*, edited by J. Messier *et al.* (Kluwer, Boston, 1988).

[45] Michael J. Fitch and Robert Osiander, Johns Hopkins APL Tech. Dig. **25**, 348 (2004).

[46] T. Kleine-Ostmann, K. Pierz, G. Hein, P. Dawson *et al.*, Electron. Lett. **40**, 124 (2004).